

On-Chip Discrimination of Orbital Angular Momentum of Light with Plasmonic Nanoslits

Supplementary Material

Shengtao Mei^{1,3*}, Kun Huang^{2*}, Hong Liu^{2*}, Fei Qin^{1*}, Muhammad Q. Mehmood¹, Zhengji Xu⁴,
Minghui Hong¹, Daohua Zhang⁴, Jinghua Teng², Aaron Danner¹, and Cheng-Wei Qiu^{1,3†}

¹Department of Electrical and Computer Engineering, National University of Singapore,
4 Engineering Drive 3, Singapore 117583, Singapore

²Institute of Materials Research and Engineering Agency for Science Technology and
Research (A*STAR), #08-03, 2 Fusionopolis Way, Innovis, Singapore 138634

³Graduate School for Integrative Sciences and Engineering, National University of Singapore,
Centre for Life Sciences (CeLS), #05-01, 28 Medical Drive Singapore 117456, Singapore

⁴Nanophotonics Laboratory, School of Electrical and Electronic Engineering, Nanyang Technological
University, Singapore 639798, Singapore

* These authors contributed equally to this work

† Correspondence and requests for materials should be addressed to C.W. Q. (email: chengwei.qiu@nus.edu.sg).

1. Side band problem:

The relative intensity of the 1st-order side band near the main focal point for each OAM state is different. It seems the magnitude of the side band will still increase for large topological charge so that it will approach the main focal spot. Actually, it is not the case. To verify this, the simulation result performed by our theoretical model is provided in Figure 1S showing the relative magnitude of the side band. It clearly shows that the magnitude of side-band reaches its maximum of ~70% at $l=10$, which is well below the normalized maximal of the main lobe. It behaves like an oscillating function after $l=10$ but never exceeds 70%.

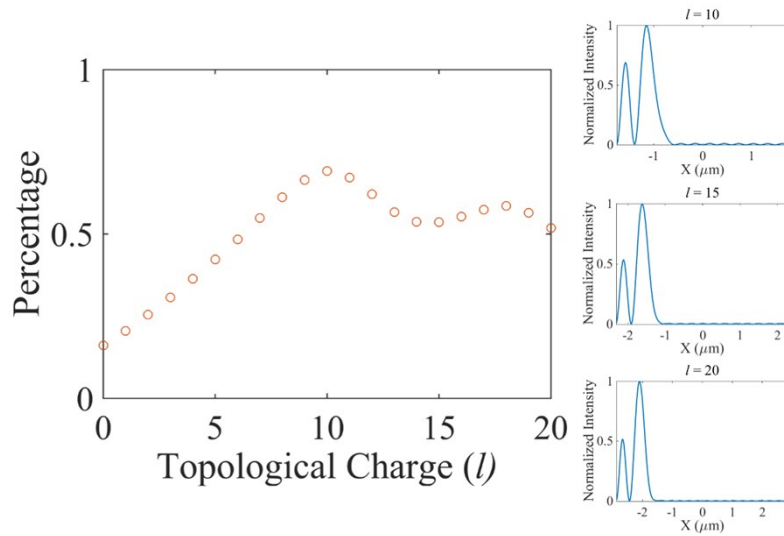


Figure 1S. Relative magnitude of the side band near the focal point. The left images show the simulated intensity distributions for the cases of $l = 10, 15, 20$.

2. Illuminating by linearly polarized LG beam

We show the experiment results of linearly polarized LG beam with $l = -5$. By considering the incident spiral phase, our model predict that the two focal spots should be at $x_1 = 480$ nm and $x_2 = 720$ nm, respectively. We show the experimental results in the Figure 2S. It clearly shows that the left circularly polarized component ($j = \sigma + l = 1 - 5 = -4$) and the right circularly polarized component ($j = \sigma + l = -1 - 5 = -6$) have their focused spots located at the right side of the center which matches well with our model. It also confirms our conclusion that the SAM can be regarded as a dc-component. Another considered issue is that linearly polarized LG beam will cause two splitting hotspots, which is not desirable in OAM state discrimination, therefore we prefer to only show fixed circularly polarized LG beam in the main text for a clear demonstration of our idea.

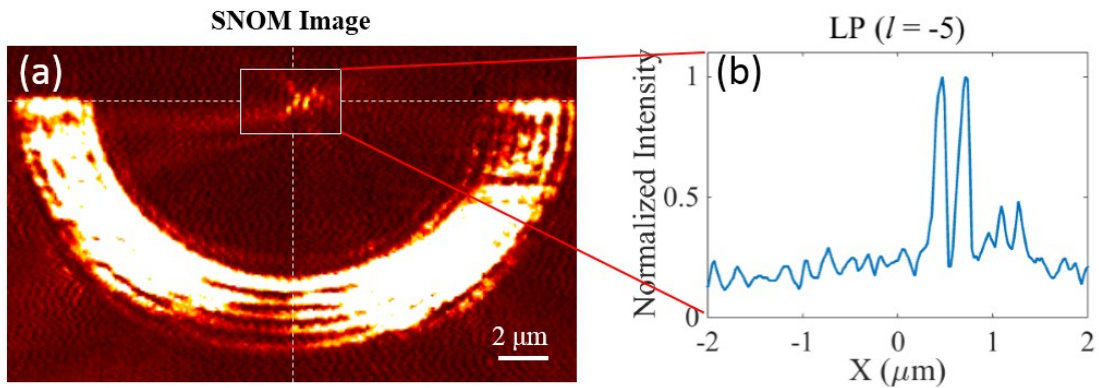


Figure 2S. Experimental results for linearly polarized LG beam with $l = -5$. (a) NSOM image of the SPPs intensity distribution. (b) Intensity distribution along the base (the horizontal white dashed line) of the slits.

3. Considering optical communication wavelength

For different working wavelengths, the period of the structure should be adjusted to the value of the corresponding SPPs wavelengths, for example, 1550 nm working wavelength means the period of the slits should be equal to its SPP wavelength of 1542 nm on the gold film. The device performance (i.e., sorting OAM) under different working wavelength will maintain. According to our analytical model, the distance between the neighboring modes for 1550nm becomes larger ($\Delta \approx 310nm$) as shown in Figure 3S.

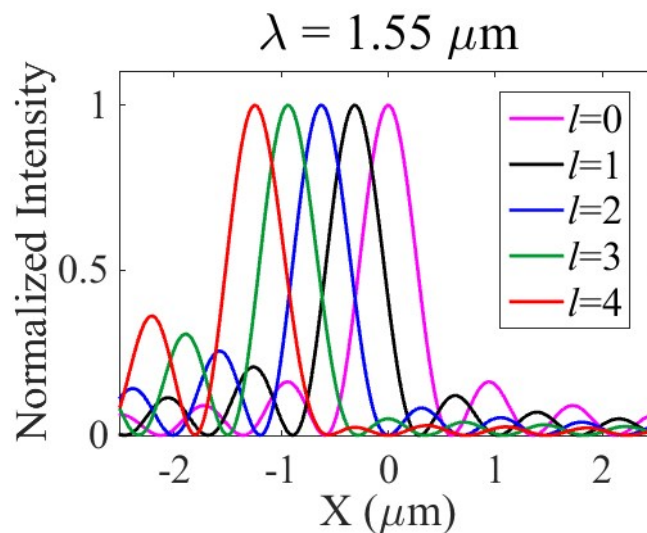


Figure 3S. Analytical model results for working wavelength $\lambda = 1.55 \mu\text{m}$.

4. Potential Strategies of reducing crosstalk

Subwavelength grooves (with 60-nm depth and 60-nm width) on the metal surface right at the focal position can be one potential strategy of reducing the crosstalk. Figure 4S shows one simulation example of this strategy.

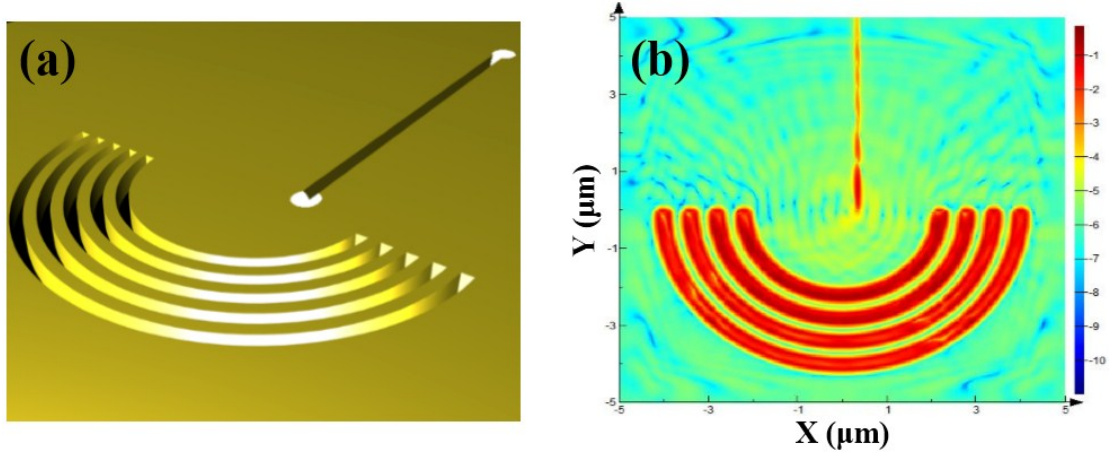


Figure 4S. (a) Illumination of the nano-sorter with one groove waveguide on the gold film. (b) E_z distribution on the gold film of the nano-sorter with a subwavelength groove on lying at $x = 240$ nm under illumination of a LG beam ($j = -2$).

Clearly, it is possible to guide SPPs away from the center. Further optimization may be required to separate different mode's SPPs with such strategy; here we just show its possibility with this example.

5. Crosstalk calculation

Here we define the neighboring main band crosstalk parameter for a certain OAM mode by

$$CT = 10 \log \left(1 - \frac{\frac{\int_{\frac{x_{l+1} + x_l}{2}}^{\frac{x_{l+1} + x_l}{2}} E_l^2 dx}{x_{l+1} + x_l}}{\frac{\int_{\frac{x_l + x_{l-1}}{2}}^{\frac{x_l + x_{l-1}}{2}} E_{l-1, l, l+1}^2 dx}{x_l + x_{l-1}}} \right) \quad (\text{dB})$$

The averaged CT for the simulated data is about -5 dB. However, if we choose interval modes like $l = 1, 4, 7, 10, \dots$, the averaged CT for the simulated data is about -12.1 dB. However, in experiment, we prefer to measure the maximum intensity value for each mode, which may further increase the precision.

6. Insertion loss of the device

Since more than half of the incident light is lost during transmission. The insertion loss for this device is relatively high and therefore energy efficiency is low. Besides, the resolution of the NSOM tip also plays an important role during this process. In our experiment, 10 mW (or even several mW) incident laser power can already excite the distinguishable focal spots on gold film surface that is measurable via the NSOM tip. For any OAM mode, the insertion loss is similar as long as the beam is properly focused to cover the structure. For fixed objective lens, larger OAM mode means larger radius, and we can employ periodic structure with adequate number of slits, for example ten slits, to cover as many modes as possible.